Multipoint Measurement Using an Inline Fibre Optic Spectrometer Fabricated with a 400 nm Femtosecond Laser

Kenji Goya[1, *], Masahiko Shiraishi[2], Atsushi Seki[3]
Kazuhiro Watanabe[3], Yusuke Fuchiwaki[1], Toshihiko Ooie[1]

[1]*Health Research Institute, National Institute of Advanced Industrial Science and Technology (AIST),*
2217-14 Hayashi-cho, Takamatsu, Kagawa 761-0395, Japan
[2]*Department of Information Systems Science, Faculty of Engineering, Soka University,*
1-236, Tangi-machi, Hachioji,Tokyo, Japan
[3]*Department of Science and Engineering for Sustainable Innovation,Faculty of Science and*
Engineering, Soka University, 1-236, Tangi-machi, Hachioji, Tokyo, Japan
[*]E-mail: k-gouya@aist.go.jp

We have demonstrated micro-hole drilling for the fabrication of an inline fibre optic spectrometer using a 400 nm femtosecond laser. An optical fibre was irradiated with a 1 kHz pulse train of 40 µJ femtosecond pulses for 1.2 s to create a through-hole that penetrates the fibre core and functions as a sample cell for spectroscopic measurements. A spiral micro-hole arrangement embedded in a multi-mode fibre provided sufficient performance for multipoint spectroscopic measurements.

1. Introduction

Over the past several decades, a wide variety of fibre optic devices have been proposed, and some have been developed sufficiently to be put into practical use. A few examples of fibre optic devices that have achieved widespread use include Mach-Zehnder [1-4] and Fabry-Perot (FP) [5-9] interferometers, fibre Bragg gratings (FBGs), [10-13], long-period fibre gratings (LPFGs) [14-17], and highly functionalized fibre optic surface plasmon resonance (SPR) sensors [18-22]. Recent interest in the field has not only been focused on the development of novel ideas but also on technologies for miniaturizing or integrating high-performance devices of various functionalities [23] onto a single optical fibre, which are sometimes referred to as "lab-on-fibre" technologies [24].

We have previously reported a new approach to the development of fibre optic inline spectroscopic device by embedding a through hole to be a sample cell in multi-mode optical fibre, using a 400 nm femtosecond laser [25, 26]. The results obtained in those studies confirmed a theoretical model describing the absorbance A_λ of a sample cell array embedded in an optical fibre. Furthermore, the findings showed that a near ultraviolet (NUV) femtosecond laser is more effective for micro-hole drilling than a near-infrared (NIR) femtosecond laser. With a NIR femtosecond laser, the processing time usually exceeds a few minutes due to the formation of laser-induced debris, and immersion oil is also required to reduce the laser-induced thermal energy [3, 27, 28]. Some of the advantages of using a NUV femtosecond laser for micro-hole drilling include a better surface roughness produced inside the sample cell (< 500 nm compared with > 1 µm for a NIR femtosecond laser), a much shorter processing time, and a significantly simpler procedure. In our previous work, we achieved efficient deep-hole drilling in very thin fibre optics with a simultaneous reduction in the amount of obstructive debris produced [26]. Additionally, the irradiation time needed to fabricate a micro sample cell for spectroscopic measurements was a very short 1.2 s.

In this study, we focus on the multipoint measurement using a single inline fibre optic spectrometer to produce a fibre optic platform which facilitates a high functionality. The sample cells were spirally arranged to obtain higher sensitivity in terms of absorbance and refractive index change, which was qualitatively predicted based on the same theoretical model used in our previous work [25, 26]. Transmission spectra were obtained using pure water to evaluate the utility of the inline fibre optic spectrometer in multipoint measurements. The results show the strong potential for these inline fibre optic spectrometers to be used in such applications.

2. Fabrication of through hole

The through-holes were fabricated as illustrated in Fig. 1. A commercially-available glass optical fibre (MMF 62.5 µm, Miki Inc.) was irradiated with 350 femtosecond pulses (λ = 400 nm) from two directions (not simultaneously) to avoid tapering of the inlet/outlet of the cell. The core and cladding diameters of the fibre were 62.5 and 125 µm, respectively. To prepare fiber optic samples, a part of the outer coating was stripped from a fiber optic cable. The length of stripped section is approximately 20 mm. The fundamental beam of a 1 kHz Ti-sapphire laser (IFRIT Cyber Laser Inc., 1 mJ/pulse, λ = 800 nm, 210 fs pulse duration) was converted to the second harmonic (240 µJ/pulse, 350 fs pulse duration) in a wavelength converter (second harmonic generation unit, SHG manufactured by Cyber Laser Inc.). The second harmonic pulses were
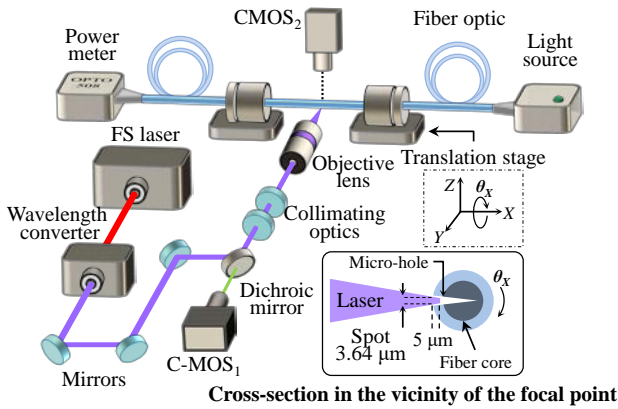
Fig. 1 Experimental apparatus for micro-hole fabrication.

introduced to an objective lens (NA = 0.28) through an optical train consisting of steering mirrors, collimating optics, an ND filter, and a dichroic mirror to focus the beam at the target optical fibre. The collimating optics reduce the beam diameter from 6.0 to 2.8 mm so that a longer Rayleigh distance compared with the initial beam can be obtained using a negative and positive lens array (Galileo configuration). The optical configuration prevents plasma generation in the air between the lens combination, which is important because the laser beam could be defocused and the energy could be lost by plasma creation during collimation and thereby affected by diffraction before the final focusing [29]. We estimate that the objective lens focuses the beam to a focal spot size of 3.64 µm, based on the effective beam diameter of 5.64 mm at the lens plane and assuming a Gaussian shape. An optical fibre was mounted on a three dimensional motor-controlled translation stage equipped with a rotary mechanism for rotation of the fibre. The transmission loss due to the through-holes was monitored as follows. 850 nm light supplied by a light source (B1385SC Dual LD, Appointech Inc.) was sent through the fibre line, and the power of the transmitted light was measured with a power meter (OP508, Opto Test Co.) after being passed through the fabricated sensor portion. The fiber sample was carefully moved and adjusted with respect to the laser focal point by moving the translation stage in the X, Y, Z and θx directions. The focal point, defined as the centre of the Rayleigh distance of 26.0 µm, was set to be 5 µm beyond the cladding surface of the inlet, corresponding to a beam diameter of 11.7 µm at the centre of the fibre core. The through-hole sample cell was designed and machined to make possible easy guidance of a liquid into the optical fibre core without the need for an immersion liquid during laser machining. The through-hole cell can be fabricated with a cell diameter of 15 µm and a taper angle of less than 1.0° at the inlet/outlet by irradiating the fibre from both sides.

3. Arrangement of cell arrays

The optimum arrangement for the cell arrays was predicted by measuring the optical transmittance T during through-hole fabrication. Both linear and spiral sample cell array configurations were evaluated, as shown in Figs. 2(a) and 2(b), respectively. The left and right panels show cross-sectional and side views of the fibre core, respectively. The factors α and α_0 respectively are the effective area ratio and

actual cross-sectional-area ratio, which are defined as the ratio of the cross-section of the sample cell S_1 to the cross-section of the entire core S_0.

The sensitivity with regard to refractive index change or absorbance A_λ measurements, depends directly on the optical path of the light transmitted through the fibre core. The transmission T can also be estimated from A_λ using the formula

$$A_\lambda = -\log_{10}(T) = -\log\left(\frac{I}{I_0}\right), \qquad (1)$$

where I_0 and I are the intensities of the incident light and total transmitted light, respectively. In general, A_λ should increase in proportion to the molar concentration c (mol/L) of the sample and the path length L (cm) according to the Lambert-Beer law
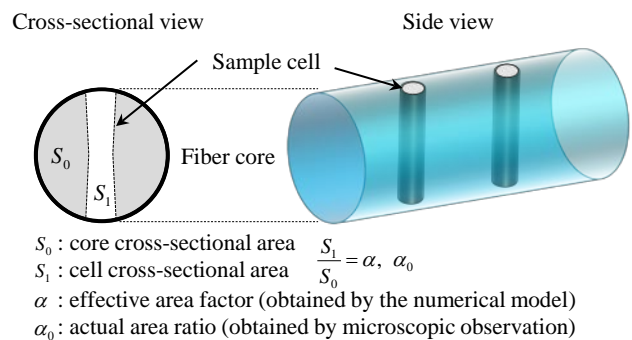
$$A_\lambda = \varepsilon_\lambda cL, \qquad (2)$$

where ε_λ (l/cm·mol) is the wavelength-dependent molar absorptivity. In order to find the ideal arrangement of the sample cells, the absorbance sensitivity of the inline fibre optic spectrometer was roughly evaluated using the numerical model [26]

$$A'_\lambda = -\log_{10}\left\{ \alpha 10^{-\varepsilon_\lambda c(n\beta L')} + (1-\alpha)\right\}, \qquad (3)$$

where n is the number of sample cells and L' is the cell diameter at the waist. The incident light I_0 should be equal to the total transmitted light I, which is the sum of the light passing through the sample cell, $\alpha I_0 10^{-\varepsilon_\lambda c(n\beta L')}$, and that remaining in the fibre core, $(1-\alpha)I_0$. As illustrated in Fig. 2, the factor α is the effective cross-sectional area ($\alpha < 1$ by definition). Even for a two-cell sensor, α for the linear arrangement is the same as that for a single cell ($\alpha_0 = 0.31$) because the cells are exactly aligned. On the other hand, for the spiral arrangement, α is larger because each cell is alternately arranged. In general, α is smaller than the ratio of the cross-section because of optical scattering at the granulated surface on cell boundaries. The factor β is the

(a) Linear arrangement (2 cells, α_0 = 0.31)

S_0 : core cross-sectional area
S_1 : cell cross-sectional area $\qquad \frac{S_1}{S_0} = \alpha, \; \alpha_0$
α : effective area factor (obtained by the numerical model)
α_0 : actual area ratio (obtained by microscopic observation)

(b) Spiral arrangement (2 cells, α_0 = 0.54)
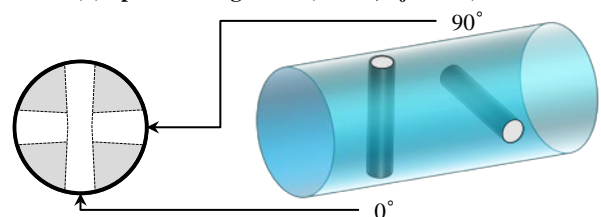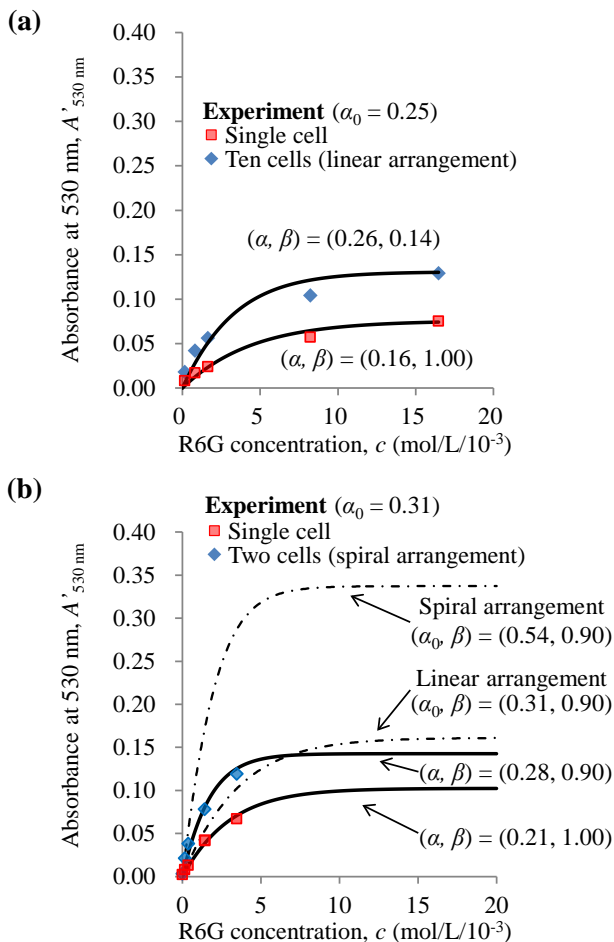

Fig. 2 Schematic cross-sectional view of sensor portions with a structural design in an (a) linear and (b) spiral cell array, where the factor α and α_0 are defined by S_1/S_0.

(a)

(b)

Fig. 3 Numerical calculation of absorbance at 530 nm as a function of Rhodamine 6G concentration, together with the experimental data (diamonds and squares) using (a) single- and ten-cell sensors, (b) single-cell and two cell for a linear and spiral arrangement. The dashed and solid lines show the numerical prediction and the model fitting.

scaling factor of path length, which is estimated from the model. The effective path length is defined as $n\beta L'$, where $\beta \leq 1$, because light travels through the round cross-section of the cylindrical cell, resulting in an overall path length that is shorter than the cell diameter at its waist. On other hand, β could be greater than 1 when the taper-angle of through-hole becomes much greater and L' should be consequently defined as the average cell diameter.

Fig. 3(a) shows a comparison of previously reported numerical calculations and experimental results [26] for a single-cell sensor and a ten-cell linear array sensor ($L' = 10$ µm, $\alpha_0 = 0.25$) using rhodamine 6G (LC5900, Lambda Physik) solutions as the absorber. Assuming an absorptivity ε_λ of 10.5×10^4 (L/mol·cm) [30] at $\lambda = 530$ nm, the calculations are in agreement with the experimental results when α and β are set to 0.16 and 1.00 and to 0.26 and 0.14 for the single-cell and ten-cell array sensor, respectively. The larger α in the latter case has been caused by an unfavourable lateral misalignment of the through-holes, which we tried to arrange as perfectly as possible along the fibre core axis during the fabrication process. On the other hand, β ($n=10$) is much smaller than 1.00, which means that a linear cell array configuration is inefficient for transmitting light to be absorbed along the entire fibre. β is inversely proportional to the number of the cells. Fig. 3(b) shows experimental results and numerical calculations corresponding to the linear and spiral arrangements shown in Figs. 2(a) and 2(b), respectively. The calculation for single cell is in agreement with the experimental result (red squares), when α and β are set to 0.21 and 1.00, respectively. By varying the cell diameter of from 10 µm in Fig .3(a) to 15 µm in Fig .3(b), the factor α increases from 0.16 to 0.21. For the absorbance of two cells with the spiral arrangement, a calculation using $(\alpha, \beta) = (0.28, 0.90)$ shows a good agreement with the experimental results (blue diamonds), where α becomes 1.3 times greater than the absorbance of single-cell sensor. The prediction was calculated assuming that α_0 equals to 0.31 and 0.54 using linear and spiral arrangement, respectively, the numerical model give higher sensitive features as dashed lines in Fig. 3(b), when $\beta = 0.90$. The prediction is in disagreement with the experimental results using a spiral cell array. To investigate absorption characteristics, using the numerical model, the half-saturation absorbance and its concentration c_{hs} were calculated and summarized in Table 1. The half-saturation absorbance of the case of using spiral arrangement is 0.071 at concentration of 1.193 mol/L/10^{-3}. Comparing with ten-cells sensor, the sensitivity in terms of the saturation absorbance and half-saturation concentration were improved, where the factor α increase slightly and β becomes much greater. The results mean that the sensitivity can be designed not only by the number of cells but also by cell arrangements and the shape of cells. Based on the results in Fig. 3, the spiral arrangement provides higher sensitivity, which is favourable for multipoint applications.
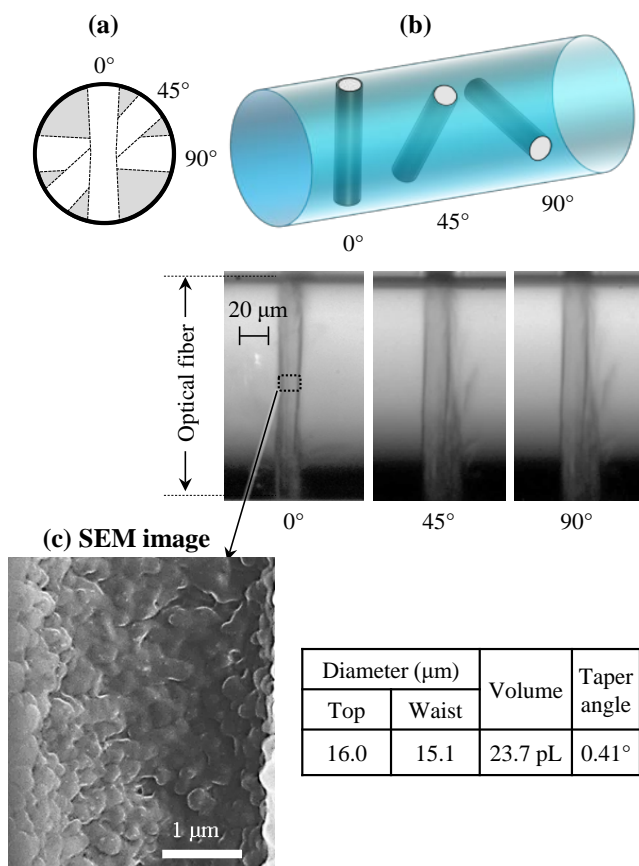
Table 1 Summary of experimental results and the model fitting.

Symbol [units]	Description	Cell arrangement			
		Linear		Spiral	
n	The number of cells	1	10	1	2
L' [µm]	Cell diameter at waist	10		15	
α	Effective cross-sectional area	0.16	0.26	0.21	0.28
β	Scale factor of path length	1.00	0.14	1.00	0.90
$A_{max}/2$	Absorbance at half-saturation concentration	0.037	0.065	0.051	0.071
c_{hs} [mol/L/10^{-3}]	Half-saturation concentration	2.98	2.26	2.08	1.19

4. Fabrication of cell arrays

The through-holes were fabricated using various second harmonic beam fluences (J/cm^2) to determine the optimal irradiation conditions that maintained the mechanical strength of the fibre line. We found that irradiating the fibre for 1.2 s using a fluence of 3.85×10^2 J/cm^2 produced the highest quality non-tapered through-holes. After producing one half of the through-hole, a second was fabricated on the opposite side of the first by rotating the mounted fibre by 180°. We confirmed that the two halves of the through-hole were connected inline using an optical microscope equipped with a CMOS sensor. The through-holes were viewed through a dichroic mirror from all directions along the circumference of the optical fibre by rotating the fibre axis. The cell array fabricated in this work was produced with an interval of 500 µm between cells.

Based on the numerical calculations discussed in Section 3, a spirally arranged through-hole array consisting of three sample cells was prepared to investigate the multipoint detection performance of the proposed fibre optic inline spectrometer. Figs. 4(a) and 4(b) respectively show cross-sectional and side view schematic diagrams of the device. The figure inset shows a side view optical micrograph taken of the sample cells, from which the average hole diameters were determined to be approximately 15.1 and 16.0 µm at the waist and surface aperture, respectively. The volume and taper angle of the through-hole were estimated to be approximately 24 pL and 0.41°, respectively, by assuming that its shape could be approximated by two truncated cones. The micrograph confirms that the through-holes were connected such that there was negligible cracking around the hole. As can be seen from Fig. 4(c), the surface roughness on the inner surface of the through-hole was confirmed to be < 500 nm using scanning electron microscopy (SEM). That NUV femtosecond laser can be used to generate through-holes with a surface roughness of approximately a few hundred nanometers is an important result of this study. It should be noted that the rugged surfaces produced with NIR light lead to more diffusive reflections, and therefore higher optical scattering. In this experiment, liquid samples were easily directed into the through-holes by capillary action, as was confirmed visually using a liquid dye. The sample cells were spirally arranged in 45° intervals to achieve higher sensitivity, as predicted by the theoretical model (see Figs. 3(a) and 3(b)) developed in [25, 26].

5. Experimental setup

As shown in Fig. 5, the experimental setup consists of a white light source (AQ-4303B, ANDO Co.) and an optical spectrum analyzer (OSA; AQ-6315, ANDO Co.) automated by a personal computer. A sensor portion of the fibre was fixed on a Teflon jig to make it easier to guide pure water into the inlet of each cell.

Spectroscopic measurements were performed with pure water to evaluate the device performance for multipoint detection. Transmission spectra were observed for different cell conditions. The three sample cells were designated Cell$_1$, Cell$_2$, and Cell$_3$ in the light source → OSA direction. Table 2 shows the status of the sample cells, where 0s and 1s are used to indicate no water or water in the cells, respectively. For example, 0-0-0 means that all three cells are empty and 1-1-1 means that all three are filled with water.
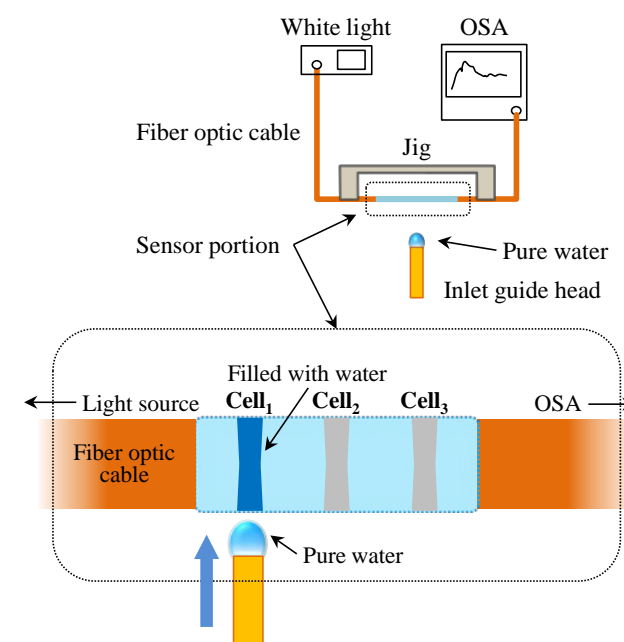

Fig. 4 Schematic diagrams of (a) cross-sectional view and (b) side view of through-holes in a spiral arrangement. The micrograph and the table show the shape and dimensions of one of the through-holes, respectively. (c) SEM image of a part of microhole.

Diameter (µm)		Volume	Taper angle
Top	Waist		
16.0	15.1	23.7 pL	0.41°

Fig. 5 Experimental setup for spectroscopic measurement

Table 2 Status of sample cells.
The 0s and 1s designate either no water or water in the sampling cells, respectively. The status 1-0-0 corresponds to the case of Fig. 5.

| Condition			Status
Cell$_1$	Cell$_2$	Cell$_3$	
1	0	0	→ 1-0-0
0	1	0	0-1-0
0	0	1	0-0-1
1	1	0	1-1-0
0	1	1	1-0-1
1	0	1	0-1-1
1	1	1	1-1-1

6. Results and discussion

Transmission losses in Cell$_1$, Cell$_2$, and Cell$_3$ (all empty) were found to be 3.11, 1.72, and 0.48 dB, respectively, which correspond to 51.1%, 32.7% and 10.5% loss. The transmission losses did not increase proportionally with the number of cells. This is because the transmission mode in the fibre core becomes weaker due to disturbance of the optical mode distribution after propagation through Cell$_1$, resulting in transmission loss at Cell$_3$ becoming much less. In our previous report, for the ten-cell array (linear arrangement), the insertion loss by the first cell was found to be almost 1.0 dB, which corresponds to approximately 20.6% loss. The other cells generated average losses of 0.07 dB each, which corresponds to only 1.60%. The transmission loss of the array used in this experiment was significantly greater due to the spiral arrangement.

To measure transmission spectra for each cell status (see Table 2), the sample cells were filled with pure water, as illustrated in Fig. 5. The results are presented in Fig. 6 as a function of wavelength. The transmission spectra are simply calculated in reference to the transmission level obtained when the cells are filled with ambient air (cell
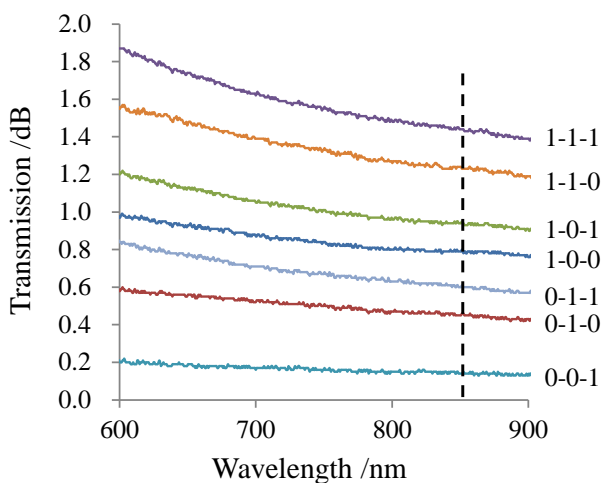
Fig. 6 Transmission spectra obtained for various cell statuses using spirally-arranged cell sensor and pure water.
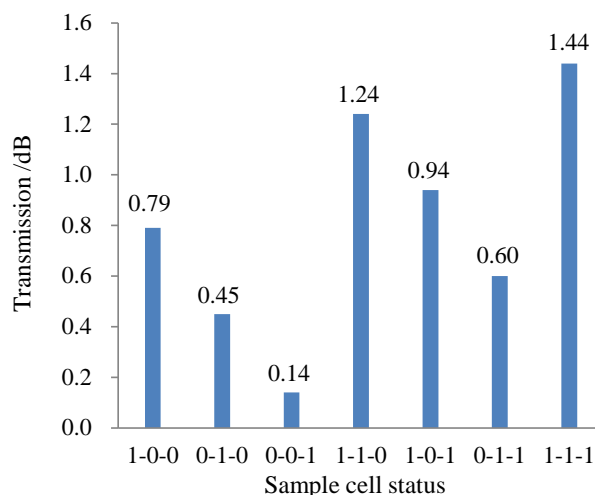
Combination	Sum		Status	
(1-0-0) + (0-1-0)	1.24		(1-1-0)	1.24
(1-0-0) + (0-0-1)	0.93	⇨	(1-0-1)	0.94
(0-1-0) + (0-0-1)	0.59		(0-1-1)	0.60
(1-0-0) + (0-1-0) + (0-0-1)	1.38		(1-1-1)	1.44

Fig. 7 Transmission change for various sample cell statuses.

status 0-0-0). As can be seen from the graph, each transmission level becomes greater than the transmission for the case of cell status 0-0-0. According to the previous study [26], it has been found that the transmission can be largely increased proportional to the refractive index inside sample cells. The spectra indicate that there is no absorption over the wavelength region focused on in this study.

The spectra in Fig. 6 show that the transmission changes over the entire wavelength range studied when the cell status is changed. The increases in transmission can be explained by Fresnel reflection that is reduced because the RI of the sample cell approaches that of the fibre core. The transmission losses measured at 850 nm for the various cell statuses are shown in Fig. 7, which were tabulated in reference to the case of ambient air. The transmission changes for 1-0-0, 0-1-0, and 0-0-1 were 0.79, 0.45, and 0.14 dB, respectively, which correspond to 16.6%, 9.80% and 3.20% recovery. For the cases of 1-1-0, 1-0-1, and 0-1-1, the transmission change increased to 1.24, 0.94, and 0.60 dB (24.8, 19.5 and 12.9%), respectively. In particular, it should be mentioned that the sum of any two of the transmission changes 1-0-0, 0-1-0, and 0-0-1 equal the corresponding loss for 1-1-0, 1-0-1, and 0-1-1. For example, the transmission change for 1-1-0 corresponds to the sum of transmission changes for 1-0-0 and 0-1-0. Similarly, the transmission change for 1-0-1 was 0.94 dB, which very nearly equals the sum of transmission changes for 1-0-0 and 0-0-1 (0.93 dB). The same was true for 1-1-1 and 1-0-0, 0-1-0, and 0-0-1.

The most important thing to note is that the status of the individual sample cells can be obtained from the spectrum baseline (if there is any absorption), which indicates that the sensing response of each cell arranged in a single fibre

optic can be clearly distinguished by observing the measured spectra.

7. Conclusions

In this study, femtosecond micro-machining was used to fabricate an inline fibre optic spectrometer by embedding a spirally-arranged micro-hole array onto commercially available multi-mode optical fibres. This arrangement was chosen based on its high sensitivity, as predicted by a theoretical model that we developed in a previous study. We then successfully demonstrated the utility of these devices for multipoint spectroscopic measurements by measuring transmission spectra of pure water.

The proposed fibre probe sensor can be used not only as a water level gauge sensor but also as a multipoint spectrometer incorporated into a single optical fibre. The cell array fabricated in this work was produced with an interval of 500 μm between cells because the original optical mode distribution can be strongly disrupted after propagation through the first cell in the array, resulting in a largely reduced central mode intensity due to the resultant scattering. The influence of such mode disruption could be reduced by choosing a longer interval between sample cells because the optical intensity of the fibre propagation mode will recover after traveling a reasonable interval due to recoupling into the propagation mode as long as the remaining beam passing through the fiber core exists. However, a longer interval in the cell array could be unfavourable for integration of the sensor into an optical fibre platform. A spiral cell array is therefore more effective for obtaining higher sensitivity. A multipoint sensing scheme can be used to perform efficient spectroscopic measurements with an extremely small amount of liquid and a very thin fibre optic platform.

References

[1] L. Zhao, L. Jiang, S. Wang, H. Xiao, Y. Lu and H. Tsai: Sensors, 11 (2011) 54.

[2] S. Zhang, W. Zhang, S. Gao, P. Geng and X. Xue: Opt. Lett. 37 (2012) 4480.

[3] Y. Wang, M. Yang, D.N. Wang, S. Liu and P. Lu: J. Opt. Soc. Am. B 27 (2010) 370.

[4] B. Li, L. Jiang, S. Wang, Q.C.M.Wang and J. Yang: Opt. Laser Eng., 50 (2012) 829.

[5] F. Xu, D. Ren, X. Shi, C. Li, W Lu, L. Lu, L. Lu, and B. Yu: Opt. Lett. 37 (2012) 133.

[6] J. Eom, C. Park, B.H. Lee, J. Lee, I. Kwon and E. Chung: Sens. Act. A 225 (2015) 25.

[7] L.H. Chen, T. Li, C.C. Chan, R. Menon, P. Balamurali, M. Shaillender, B. Neu, X.M. Ang, P. Zu, W.C. Wong and K.C. Leong, Sens. Act. B 169 (2012) 167.

[8] F. C. Favero, L. Araujo, G. Bouwmans, V. Finazzi, J. Villatoro and V. Pruneri: Opt. Lett. 20 (2012) 7112.

[9] J. Li, X. Qiao, R. Wang, Q. Rong, W. Bao, Z. Shao, T. Yang: Opt. Laser Eng. 79 (2016) 16.

[10]G. D. Marshall., R.J. Williams, N. Jovanovic, M.J. Steel and M.J. Withford: Opt. Exp. 18 (2010) 19844.

[11]P. C. Hill, G. R. Atkins, J. Canning, G. C. Cox and M. G. Sceats: Appl. Phys. 33 (1995) 7689.

[12]M. L. Åslund, N. Jovanovic, N. Groothoff, J. Canning, G. D. Marshall, S.D. Jackson, A. Fuerbach and M.J. Withford: Opt. Exp. 16 (2008) 14248.

[13]J. U. Thomas, N. Jovanovic, R. G. Kr¨amer, G. D. Marshall, M. J. Withford, A. T¨unnermann, S. Nolte and M.J. Steel: Opt. Exp. 20 (2012) 21434.

[14]A.M. Vengsarkar, P.J. Lemaire, J.B. Judkins, V. Bhatia, T. Erdogan, and J.E. Sipe: J. Lightwave Technol. 14 (1996) 58.

[15]X. Sun, P. Huang, J. Zhao, L. Wei, N. Zhang, D. Kuang and X. Zhu: Front. Optoelectron. 5 (2012) 334.

[16]B. Li, L. Jiang, S. Wang, H. Tsai and H. Xiao: Optics Laser Technol. 43 (2011) 1420.

[17]T. Allsop, M. Dubov, A. Martinez, F. Floreani, I. Khrushchev, D.J. Webb and I. Bennion: J. Lightwave Technol. 24 (2006) 3147.

[18]R. Slavı́k, J. Homola and E. Brynda: Biosens. and Bioelectron. 17 (2002) 591.

[19]C.H. Chen, T.C. Tsao, W.Y. Li, W.C. Shen, C.W. Cheng, J.L. Tang, C.P. Jen, L.K. Chau and W.T. Wu: Microsyst. Technol., 16 (2010) 1207.

[20]C.H. Chen, T.C. Chao, W.Y. Li, W.C. Shen, C.W. Cheng, J.L. Tang, L.K. Chau and W.T. Wu: J. Laser Micro/Nanoeng., 5 (2010) 1.

[21]A. Hosoki, M. Nishiyama, H. Igawa, A. Seki, Y. Choi and K. Watanabe: Sens. Act. B 185 (2013) 53.

[22]M.C Hsieh, Y.H. Chiu, S.F. Lin, J.Y. Chang, C.O. Chang and H.K. Chiang: Sensors 15 (2015) 3565.

[23]Y. Cheng, K. Sugioka, K. Midorikawa: Opt. Express. 12 (2005) 7225.

[24]M. Consales, M. Pisco and A. Cusano, Lab-on-Fiber Technology: a New Avenue for Optical Nanosensors, Photonic sensors 2 (2012) 289.

[25]K. Goya, T. Itoh, A. Seki and K. Watanabe: EUROSENSORS 2014, the XXVIII edition of the conference series. Procedia Engineering B4P-E06-5074.

[26]K. Goya, T. Itoh, A. Seki and K. Watanabe: Sens. Act. B 210 (2015) 685.

[27]R. Buividas, M. Mikutis, G. Gervinskas, D. Day, G. Slekys and S. Juodkazis: Nanoengineering: Fabrication, Properties, Optics, and Devices IX, Proc. of SPIE 8463 (2012) 84630T1.

[28]Y. Wang, D.N. Wang, M. Yang, W. Hong and P. Lu: Opt. Lett. 34 (2009) 3280.

[29]M. Mlejnek, E.M. Wright and J.V. Moloney: Opt. Lett. 23 (1998) 382.

[30]U. Brackmann, Lamdachrome laser dyes data sheets 3rd edition, Lamda Physik, Göttingen (2000).